

MAGIC-f Gel Dosimeter Reading: A Comparison between an In-House Optical CT and MRI Imaging

Zahra Mansouri¹, Ahmad Mostaar^{1,2*}, Mahmoud Shiri¹, Mohsen Sadat-Shahabi¹

1. Department of Medical Physics and Biomedical Engineering, School of Medicine, Shahid Beheshti University of Medical Sciences, Tehran, Iran
2. Radiation Biology Research Center, Iran University of Medical Sciences, Tehran, Iran

ARTICLE INFO	ABSTRACT
<p>Article type: Original Paper</p> <hr/> <p>Article history: Received: Jul 07, 2020 Accepted: Oct 22, 2020</p> <hr/> <p>Keywords: Optical Tomography Radiometry MAGIC Polymer Gel Magnetic Resonance Imaging Radiotherapy</p>	<p>Introduction: According to new developments in radiation therapy techniques, accurate dose verification in three dimensions has become more critical. Polymer gel dosimeters (PGDs) are valuable tools to be used for this purpose. Nowadays, various imaging modalities are employed to read out the gels. This study was aimed to investigate the measured dose distribution recorded in MAGIC-f PGD with optical computed tomography (OCT) by comparison with MRI.</p> <p>Material and Methods: We developed an in-house charge-coupled device (CCD) based cone-beam OCT scanner. A phantom of MAGIC-f PGD was used to measure a four-field box dose distribution. MRI and OCT scanners were performed for gel readouts. Both measurement results were compared by gamma index analysis with various acceptance criteria. The temporal stability of the gel was also evaluated with the OCT readout system.</p> <p>Results: The percentage of isodose lines from two measured datasets agreed well together. The pass rates were 99.02%, 96.8%, and 89.8% with 5%/5mm, 4%/4mm, and 3%/3mm criteria, respectively, at the phantom's central axial slice.</p> <p>Conclusion: The results indicate that the performance of this OCT system is almost the same with acceptable discrepancies to the MRI as accepted standard readout modality, and it can be used for three-dimensional dose verifications.</p>
<p>► Please cite this article as: Mansouri Z, Mostaar A, Shiri M, Sadat-Shahabi M. MAGIC-f Gel Dosimeter Reading: A Comparison between an In-House Optical CT and MRI Imaging. Iran J Med Phys 2021; 18: XX-XX. 10.22038/IJMP.2021.53179.1876.</p>	

Introduction

In recent decades, modern high gradient radiotherapy techniques such as intensity-modulated radiation therapy (IMRT), stereotactic body radiotherapy (SBRT), and Stereotactic Radiosurgery (SRS) have been developed increasingly to deliver a uniform prescribed dose with a small margin to the target volume while sparing surrounding healthy tissues [1]. Accurate 3D dose verification is essential in these techniques and can influence the quality of treatment [2, 3].

The verifying of such accuracies with conventional dosimeters is very challenging because these dosimeters are only able to measure the dose in single points or two-dimensional planes [4-7]. However, some commercial companies like PTW [8], Scandi-Dos [9, 10], and Sun Nuclear [11, 12] have produced phantoms as false 3D dosimeters. The detectors used in these phantoms are diode arrays or ionization chambers with a 4-10 mm center to center distance. Therefore, in high-dose gradient regions, the performance of these dosimeters has a notable error [13, 14]. Gel dosimeters, including Fricke gel dosimeters, and polymer gel dosimeters (PGDs), are

valuable tools for recording the dose distribution in fully three-dimensions. Fricke gels are based on converting the ferrous (Fe^{2+}) to ferric (Fe^{3+}) ion upon irradiation. However, Ferric ion diffusion in the gel is a significant limitation for the use of the Fricke gels. PGDs work based on monomer conversion to polymer and cross-linking upon irradiation. PGDs are tissue equivalent, have a high spatial resolution, and overcome the diffusion problem in Fricke gels [5, 15, 16]. Furthermore, the use of a radiochromic solid polymer dosimeter named PRESAGE has increased recently for three-dimensional dosimetry [17]. Some studies have shown that this type of solid polymer has good dosimetric properties and physical properties for use in radiotherapy dosimetry [18, 19]. The various changes caused by radiation absorption in gel dosimeters appropriate them to readout with imaging modalities, including magnetic resonance imaging (MRI) [20, 21], X-ray Computed tomography (x-ray CT) [22], Optical Computed tomography (OCT) [23], Ultrasound [24, 25], and Spectrophotometry [26]. MRI is the first and the gold standard readout method [20].

However, MRI disadvantages, such as being expensive, time-consuming, lack of MRI scanners in most radiotherapy clinics, had led to notice researchers' attention to the other readout methods of gel dosimeters [23, 27, 28]. Among the many studies that were performed to replace MRI with the other readout methods, OCT has been very popular. This modality was first introduced in the mid-1990s and operated based on mapping the light attenuation coefficients of the irradiated gel [23,29]. This readout tool is low-cost, compact, and has higher sensitivity and signal to noise ratio (SNR) [28, 30, 31]. However, artifacts that arise from refraction and reflection of the light can affect the quality of its images [31].

The current study aimed to compare the dose distributions recorded in a polymer gel dosimeter reading by our in-house CCD-based cone-beam OCT scanner and MRI (as gold standard). For this purpose, a MAGIC-f PGD was used along with our OCT and an MRI scanner to perform the dose distribution measurement. Then the results of the two measurements were compared together by gamma analysis.

Materials and Methods

Gel preparation

The MAGIC-f PGD was selected for this study because of its characteristics of a high melting point (69°C), and high sensitivity to irradiation due to the presence of formaldehyde in its formulation. These benefits are important because they ensure spatial information preservation and make the polymer gel easy to maintain and control [32]. Besides, MAGIC-f can be used along with the OCT scanner because it has a transparent optical structure. MAGIC-f gel dosimeter was manufactured according to Fernandez et al. [32]. The composition in the mass concentration used in this study is shown in Table 1. The gel solution was then poured into an acrylic cylindrical phantom with 6 cm diameter, 6.5 cm height, 0.5 cm wall thickness, and calibration vials with 1.5 cm diameter and 10 cm height. Parafilm tape was used to prevent oxygen penetration, and aluminum foil was wrapped around the phantom and vials to neutralize the effect of photopolymerization. Then the vials and phantom stored in a refrigerator at 4° C for 24 hours before measurements.

Table 1. MAGIC-f gel components and concentrations

Component	Mass concentration (%)
Mili-Q water	82.31
Porcine skin gelatin-300 bloom (SIGMA-ALDRICH®)	8.33
Methacrylic acid 99%(Merc®)	5.99
Formaldehyde, a water solution with 37% minimum and stabilized with 10-15% methanol (SIGMA-ALDRICH®)	3.32
Ascorbic acid 99% (Acros®)	0.03
Copper (II) sulfate.5H ₂ O(Merc®)	0.02

Treatment Planning and dose delivery

The gel phantom was transferred to the x-ray CT simulation room two hours before irradiation to equilibrate with CT room temperature (20 °C). The phantom was placed horizontally on a Perspex stand with a height of 12.5 cm, which was designed to hold the phantom in a precise alignment. It was placed in the center of a 25x25x35 cm³ Perspex water tank, and the central horizontal plane of the cylinder was at a depth of 10 cm of water. The CT images of the gel phantom were acquired using the Siemens CT scanner (SOMATOM emotion, Germany). The CT data set was exported to the treatment planning system (TPS) (Isogray, Edition 4.2.3.63L, Dosisoft, France) to generate a 6 MV X-ray photon 4-field box plan. A 6 Gy dose was prescribed to the isocenter point (the center of the gel phantom). The calibration vials, which were placed at 3cm depth of the 25x25x35 cm³ water tank (the distance from the central plane in vials to the outer edge of the water tank was 3cm, i.e., SSD=97cm), were irradiated using 20x20 cm², 6 MV photon beam in the dose range of 0 as a control to 10 Gy, while the gantry angle was 90 degree. The gel phantom was irradiated exactly like under CT simulation set-up conditions using the linear accelerator (Elekta Compact model). The gantry angles were 0, 90, 180, 270 degrees, the SSDs were 90, 87.5, 89, 87.5 cm, respectively, and the field size was 4*4cm². Figure 1 shows the irradiation set-up of vials and the phantom.

Imaging

Twenty-four hours after irradiation and completion of the polymerization procedure, imaging was performed to read out the gels.

Optical CT scanner imaging

We developed an in-house CCD-based cone-beam OCT scanner to gel dosimetry readout [33]. Figure 2 shows the geometry of the scanner schematically. In this scanner, a LED array source (a) emitted visible light with 600 nm wavelength. After passing through a thin diffuser sheet and the refractive index matching water-filled tank (c), this light reaches a CCD-camera (f) (TUCSEN- H series-with a 12.5 mm focal length lens).

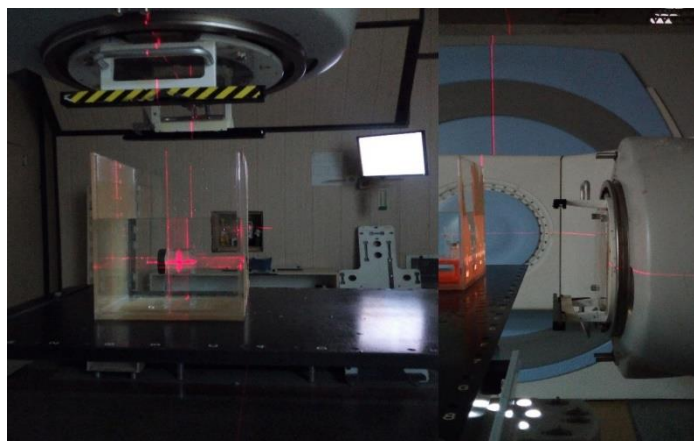


Figure 1. The phantom (left) and calibration vials (right) set up inside the water tank prepared for irradiation.

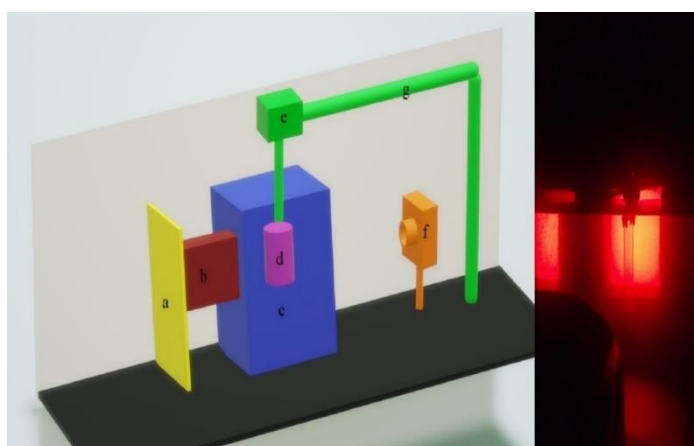


Figure 2. Left) Three-dimensional schematic geometry of optical CT scanner. a) LED array source b) diffuser in a collimator c) water tank d) gel phantom e) stepper motor f) CCD-camera g) L arm. Right) a calibration vial during the optical CT scanning

The imaging FOV was limited using a rectangular collimator (b) placed between the source and the water tank. The gel container (d) was placed at the center of the water tank and attached to a stepper motor (e) that controlled its rotational movements. The scanner warm-up was performed for two hours before imaging. Two hundred projections were acquired in 360° with 1.8° step increments. After scanning, image reconstruction was performed using an in-house filtered back-projection algorithm written in MATLAB (Math Works Inc., Natick, MA, USA).

MR-imaging

We also used MRI modality to compare the dose distribution recorded in the MAGIC-f PGD on the same day with optical imaging. For this purpose, 3 Tesla MRI Scanner (GE, DISCOVERY MR750W, USA) and the standard head coil were used. The imaging protocol used in this study is as follows: 16 echoes with TE= 22.5- 360ms, TR= 3000ms, FOV=250 mm², matrix size=128*128 voxels, NEX=2, and slice thickness =3mm.

Data analysis

The following steps were performed to obtain the calibration curves for the MAGIC-f gel. Doses of 0.5, 1,

2, 4, 6, 8, and 10 Gy were delivered to 7 cylindrical calibration vials, and the samples were scanned by MRI and OCT. The average R2 values and attenuation coefficients were calculated in the axial slices of MRI images and OCT reconstructed images, respectively. Then the calibration curves were plotted based on the obtained data.

Registration of OCT and MRI dose maps and gamma analysis

After MRI and OCT scanning the phantom, the dose maps were extracted for both images; then, the OCT data were compared with the MRI data as the reference using an in-house MATLAB code. For comparing purposes, the dose images from two modalities have been registered on each other. In order to be more accurate in the registration process, we chose three different points on the inner and outer edges of the phantom, randomly at axial, coronal, and sagittal planes, and the registration was performed based on the matching of the edges at the location of those points. . Then, interpolation was needed to resize the images since the pixel size of the OCT and MRI volume data were not equal. To decrease the oxygen penetration effects, only 80% of central data inside the axial slice of the phantom image was used, and the outer 20%, and

edges, were removed. As more explanation, the presence of oxygen molecules can inhibit the radiation-induced polymerization process in the PGDs. These molecules can be driven into the container of the gel and adhere to the phantom walls during pouring the liquid gel into the container or penetrating through the walls, inevitably. Therefore, the dose distribution near the container walls is not reliable [34]. So, for more accuracy, we exclude the near-wall dose distribution data from our study. The gamma analysis is commonly used for a quantitative comparison between a reference and evaluated dose distribution based on dose difference (DD) and spatial inaccuracy (Distance to agreement, DTA)[35, 36].

In this study, the MRI was used as a reference and compared to the OCT dose map of the MAGIC-f gel dosimeter. 2-D gamma analysis of the central axial slice was carried out using an in-house MATLAB code. This code used the gamma equation and the MRI and OCT dose maps were used as input images and it generated the gamma image with DD and DTA criteria of 3%/3mm 4%/4mm, and 5%/5 mm.

A) optical temporal stability

Formaldehyde, as one of the MAGIC-f gel dosimeter components, increases the temporal stability of the gel by raising the melting point of the gel to 69°C. So the optical temporal stability of the gel was measured for three weeks. For this purpose, we used the irradiated

vials with doses of 2,6 and 10 Gy and scanned them 24 hours after irradiation and then weekly for three weeks.

Results

As demonstrated in Figure 3, the calibration curves for both measurement methods show a linear relationship between R2 or attenuation coefficient values and doses, which provided all the R2 or optical attenuation distributions to be normalized based on isocenter dose values. The results showed linear dose responses up to the maximum delivered dose that was 10 Gy.

Figure 4 shows the axial central slice dose map distributions of the MRI and OCT after interpolation and registration. Some isodose curves extracted from two methods are presented in Figure 4 for visual evaluation of agreement.

Figure 5 shows the results of the 2D gamma evaluation comparison between the central axial slice of the MRI and the OCT dose distributions of the MAGIC-f gel dosimeter. Table 2 shows the pass rates of gamma evaluation between MRI and OCT dose distributions at a depth of 30 (central axial slice), 40 and 50 mm of the phantom with 3%/3mm, 4%/4mm, and 5%/5mm acceptance criteria. Gamma histograms are shown in Figure 6 for three acceptance criteria. These histograms show the frequencies of pixels that have a certain amount of gamma value.

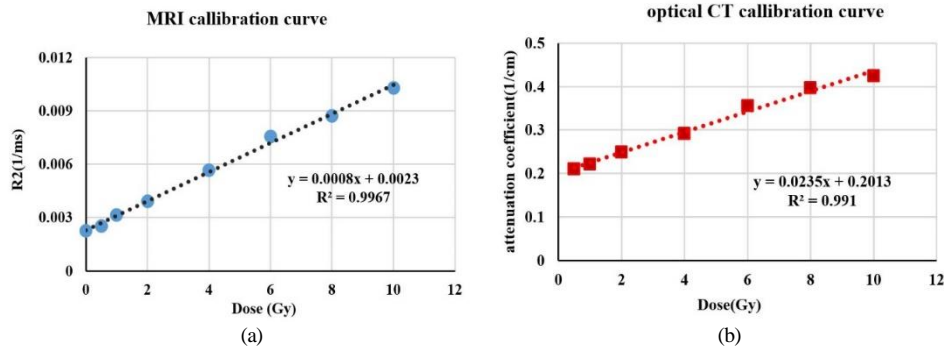


Figure 3. The curves represent the calculated R2 values and attenuation coefficients versus the corresponding doses in the MAGIC-f gel (a) MRI and (b) OCT calibration experiments. The dotted lines represent the linear regression of plotted points

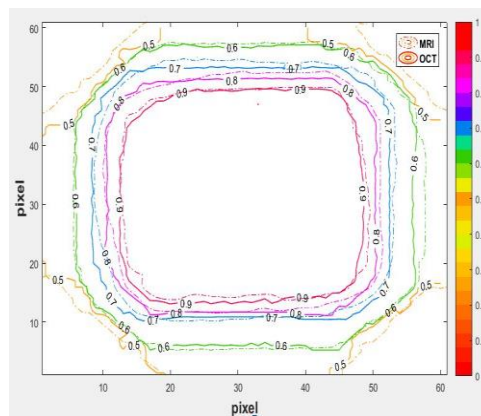


Figure 4. Comparison of registered isodose curves from the central axial slice of MRI and OCT dose map images

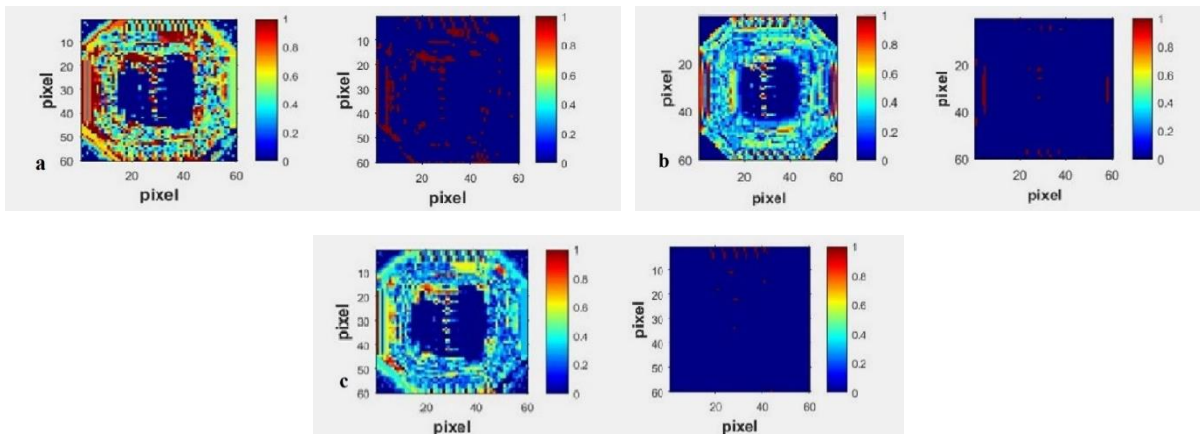


Figure 5. 2-D gamma analysis results for the axial central slice of MRI dose distribution and the OCT dose distribution of MAGIC-f gel dosimeter using the criteria of a) 3%/3 mm, b) 4%/4mm, and c) 5%/5mm. The left column shows gamma index maps, and the right one shows passing and rejected pixels in blue and red, respectively

Table 2. Gamma evaluation pass rates (%) for different depths of phantom (30, 40, 50mm) with three acceptance criteria (DD (%)/DTPA (mm)) 3%/3mm, 4%/4mm and 5%/5mm

Depth of phantom (mm)	3%/3mm	4%/4mm	5%/5mm
30 (isocenter)	89.8	96.8	99.02
40	89.3	96.3	99
50	85.3	90	91.2

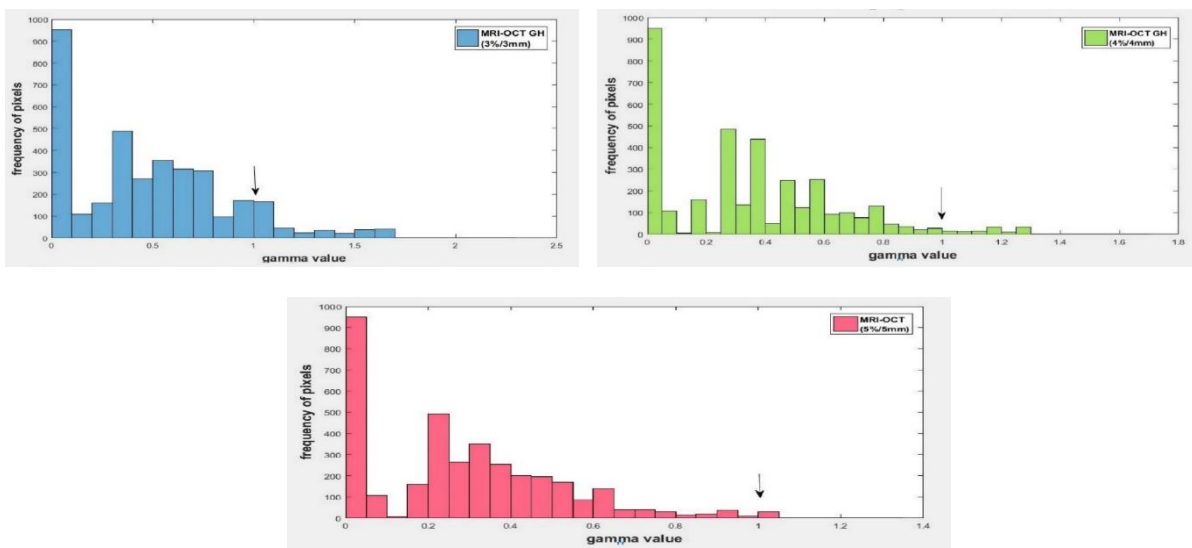


Figure 6. Gamma histograms for comparison between MRI and OCT dose distributions with acceptance criteria of 3%/3mm (blue), 4%/4mm (green), and 5%/5 mm (red). The indicator on the picture shows the reference line where the gamma evaluation test accepted the pixel value

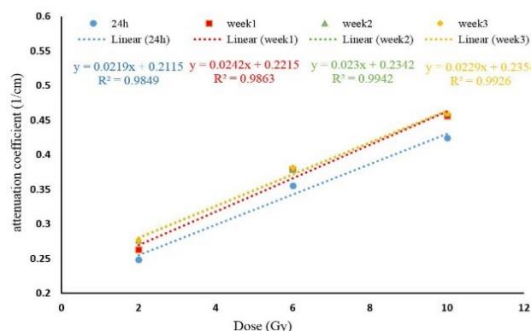


Figure 7. the calibration curves of irradiated vials with doses of 2, 6, and 10 Gy, which were scanned by OCT system 24 h and three weeks (weekly) after the irradiation to assess the temporal stability of optical response of gel dosimeter

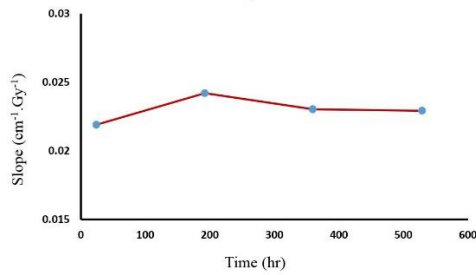


Figure 8. The slope of the calibration curve vs. the time after irradiation to evaluate the optical temporal stability

Figure 7 presented the calibration curves for irradiated vials with doses of 2, 6, 10 Gy after 24 hours of irradiation. Three consecutive weeks (weekly) were drawn to assess the optical temporal stability of the gel dosimeter. Figure 8 shows the slope of OCT calibration curve equations in terms of hours after irradiation to evaluate the optical response changes over time.

Discussion

As demonstrated in Figure 4, there is a good agreement between OCT and MRI, which is considered as the gold-standard method to readout gel dosimeters [20]. More disagreements are related to areas with lower dose levels adjacent to the phantom walls. In OCT images, these areas are very susceptible to reflection and refraction artifacts [31]. According to Figure 5 and Table 2, based on gamma analysis performed with different pass rate criteria, the most disagreements are observed at a depth of 50 mm of the phantom, especially for the 3%/3mm criterion. It is related to the high gradient dose region due to proximity to the radiation field's edge. However, beyond this, air penetration might also have another negative effect due to the diffusion of oxygen in the gel in such areas that are close to the end part of the phantom or gel container. These results were consistent with the obtained results from the studies conducted by Awad et al. [37], Pavoni et al. [38].

Compared with the previously published studies that have used the other gel dosimeters and performed gamma evaluation comparison between treatment planning calculations and imaging measurements [37-41], in the current study, the gamma evaluation comparison was conducted between two measurements

data, i.e., MRI and OCT. the advantages of this comparison are eliminating the TPS calculation errors and registration deviations due to differences in TPS computational grid size and MRI resolution. Beyond that, the gel dosimetry process, including gel manufacturing, environmental conditions, phantom set-up errors during the irradiation, and dose delivery, were the same in both measurements, and only the readout method was different. However, as detailed in Table 3, the agreement level in the current research is comparable or better to that of others. In a comparison of the treatment planning calculation and OCT dose distribution data, Yao et al. achieved the pass rates of 99.5% and 97.8% with 5%/5mm and 4%/4mm criteria, respectively[39]. Our yielded pass rates of 99.02% and 96.8% with the same criteria are comparable with their results. While our results are more reliable than the study of Oldham et al. [40], Chang et al. [41], and Pavoni et al. [38].

Previously published literature has reported an in-house OCT capability to read out the calibration vials of MAGIC-f gel dosimeter as a proof of concept [42]. However, in that study, MRI and OCT were not directly compared in assessing any dose distribution. Our study has compared dose distribution images acquired from two imaging modalities by gamma evaluation method; It has revealed more completed and precise information about the dose distribution recorded in an irradiated phantom by four field-box.

Regarding the optical temporal stability, as shown in Figure 7, the lowest response is observed 24 hours after the irradiation. The response of the other weeks almost overlaps, indicating the appearance of stability in the gel's response. As presented in Figure 8, the variation of the slopes revealed that our OCT scanner has the capacity and adequate sensitivity to record the trend of temporal stabilization in the MAGIC-f gel dosimeter comparable to the other studies that used MRI.

In this study, the slopes of the OCT calibration curves have changed from the lowest ($0.02194 \text{ cm}^{-1}.\text{Gy}^{-1}$) in the first week, then 0.02416 , 0.02295 , and $0.02291 \text{ cm}^{-1}.\text{Gy}^{-1}$ in the consequence weeks. This trend is similar to the results obtained by Pavoni et al.[43] for MRI calibration curve slopes that have changed from $0.46 \text{ s}^{-1}.\text{Gy}^{-1}$ in the first week to 0.53 , then 0.5 in the consequence weeks.

Table 3. A comparison between our results and previous studies in detail. The type of gel, the readout (imaging) system, and gamma analysis pass rates with the relevant criteria are presented in each study.

Author. Year	Irradiation technique	PGD	Readout system	reference	Criteria	Pass-rate
Oldham et al.2004[40]	IMRT	---	In-house OCT	TPS	4%/3 mm	96%
Pavoni et al. 2012[38]	Tomotherapy	MAGIC-f	MRI	TPS	3%/3mm 4%/4mm	88.4% 96.5%
Yao et al.2012[39]	IMRT	NIPAM	Commercial OCT (OCTAPU)	TPS	3%/3mm 4%/4mm 5%/5mm	92.1% 97.8% 99.5%
Chang et al. 2013[41]	4-field box	NIPAM	In-house OCT	TPS	4%/4mm	94-95%
The current study	4-field box	MAGIC-f	In-house OCT	MRI	3%/3mm 4%/4mm 5%/5mm	89.8% 96.8% 99.02%

Conclusion

We developed an OCT system and scanned the MAGIC-f gel dosimeter by this scanner and MRI. There was a linear correlation between the R2 values derived from MRI and the dose. Also, there was an acceptable linear correlation between the attenuation coefficient derived from OCT and the dose value. A comparison by gamma analysis of measured dose distributions of MAGIC-f gel dosimeter by OCT and MRI resulted in a good agreement with satisfactory preservation of gel's optical response overtime after irradiation. This in-house OCT system can be used for gel dosimetry in further researches and by some considerations in clinical evaluations.

Acknowledgment

This article was derived from the M.Sc. thesis of Zahra Mansouri in the Medical Physics Department at the Shahid Beheshti University of Medical Sciences. (Registration No:390).

References

- Schreiner LJ. Fundamentals of 3D dosimetry. In *Journal of Physics: Conference Series* 2019 Aug 1 (Vol. 1305, No. 1, p. 012022). IOP Publishing.
- Haraldsson P, Karlsson A, Wieslander E, Gustavsson H, Bäck SÅ. Dose response evaluation of a low-density normoxic polymer gel dosimeter using MRI. *Physics in Medicine & Biology*. 2006 Feb 1;51(4):919.
- Novotný Jr J, Spěváček V, Dvořák P, Novotný J, Čechák T. Three-dimensional polymer gel dosimetry: basic physical properties of the dosimeter. *Radiation Physics and Chemistry*. 2001 Jun 1;61(3-6):255-8.
- Basfar AA, Moftah B, Rabaeh KA, Almousa AA. Novel composition of polymer gel dosimeters based on N-(Hydroxymethyl) acrylamide for radiation therapy. *Radiation Physics and Chemistry*. 2015 Jul 1;112:117-20.
- Turonok OC, Diachenko O, Alokхина MY, Bezshyyko O, Golinka-Bezshyyko L, Kadenko I, et al. Three-dimensional Polymer Dosimetry. WDS'13 Proceedings of Contributed Papers, Part III, 2013.58-61.
- Maryanski MJ, Audet C, Gore JC. Effects of crosslinking and temperature on the dose response of a BANG polymer gel dosimeter. *Physics in Medicine & Biology*. 1997 Feb;42(2):303.
- De Deene Y. Review of quantitative MRI principles for gel dosimetry. In *Journal of Physics: Conference Series* 2009 May 1 (Vol. 164, No. 1, p. 012033). IOP Publishing.
- Van Esch A, Clermont C, Devillers M, Iori M, Huyskens DP. On-line quality assurance of rotational radiotherapy treatment delivery by means of a 2D ion chamber array and the Octavious phantom. *Medical physics*. 2007 Oct;34(10):3825-37.
- Nilsson G. SU-FF-T-135: Delta4-A New IMRT QA Device. *Medical Physics*. 2007 Jun;34(6Part9):2432.
- Nilsson J, Hauer AK, Bäck A. IMRT patient-specific QA using the Delta4 dosimetry system and evaluation based on ICRU 83 recommendations. In *Journal of Physics: Conference Series* 2013 Jun 26 (Vol. 444, No. 1, p. 012048). IOP Publishing.
- Létourneau D, Publicover J, Kozelka J, Moseley DJ, Jaffray DA. Novel dosimetric phantom for quality assurance of volumetric modulated arc therapy. *Medical physics*. 2009 May;36(5):1813-21.
- Yan G, Lu B, Kozelka J, Liu C, Li JG. Calibration of a novel four-dimensional diode array. *Medical physics*. 2010 Jan;37(1):108-15.
- Pavord D. SU-GG-T-210: A Comparison of Dosimetry Devices. *Medical Physics*. 2008 Jun;35(6Part12):2773-4.
- Penn ST, Xue T. SU-GG-T-170: Using a 3D Diode Array System to Perform Routine IMRT Machine QA. *Medical Physics*. 2008 Jun;35(6Part11):2765-.
- Hayati H, Mesbahi A. Impact of photon spectra on the sensitivity of polymer gel dosimetry by X-ray computed tomography. *Iranian Journal of Medical Physics*. 2019;16(1):48-55.
- Gore JC, Kang YS. Measurement of radiation dose distributions by nuclear magnetic resonance (NMR) imaging. *Physics in Medicine & Biology*. 1984 Oct;29(10):1189.
- Adamovics J, Maryanski M. New 3D radiochromic solid polymer dosimeter from leuco dyes and a transparent polymeric matrix. *Medical Physics*. 2003 Jun;30(6).
- Mostaar A, Hashemi B, Zahmatkesh MH, Aghamiri SM, Mahdavi SR. A basic dosimetric study of PRESAGE: the effect of different amounts of fabricating components on the sensitivity and stability of the dosimeter. *Physics in Medicine & Biology*. 2010 Jan 14;55(3):903.
- Mostaar A, Hashemi B, Zahmatkesh MH, Aghamiri SM, Mahdavi SR. Development and characterization of a novel PRESAGE formulation for radiotherapy applications. *Applied Radiation and Isotopes*. 2011 Oct 1;69(10):1540-5.
- Baldock C, Burford RP, Billingham NC, Cohen D, Keevil SF. Polymer gel composition in magnetic resonance imaging dosimetry. *Med. Phys.* 1996;23:1070.
- Maryanski MJ, Eastman P, Holcombe SD, Avison RG, Zhang Y, Gore JC. 122 Three dimensional visualization and measurement of conformal dose distributions using magnetic resonance imaging of bang polymer gel dosimeters. *International Journal of Radiation Oncology, Biology, Physics*. 1995(32):202.
- Hilts M, Audet C, Duzenli C, Jirasek A. Polymer gel dosimetry using x-ray computed tomography: a feasibility study. *Physics in Medicine & Biology*. 2000 Sep 1;45(9):2559.
- Gore JC, Ranade M, Maryanski MJ, Schulz RJ. Radiation dose distributions in three dimensions from tomographic optical density scanning of polymer gels: I. Development of an optical scanner. *Physics in Medicine & Biology*. 1996 Dec;41(12):2695.
- Mather ML, Whittaker AK, Baldock C. Ultrasound evaluation of polymer gel dosimeters. *Physics in Medicine & Biology*. 2002 Apr 19;47(9):1449.
- Mather ML, Charles PH, Baldock C. Measurement of ultrasonic attenuation coefficient in polymer gel dosimeters. *Physics in Medicine & Biology*. 2003 Sep 30;48(20):N269.

26. Baldock C, Rintoul L, Keevil SF, Pope JM, George GA. Fourier transform Raman spectroscopy of polyacrylamide gels (PAGs) for radiation dosimetry. *Physics in Medicine & Biology*. 1998 Dec;43(12):3617.
27. Mesbahi A, Zakariaee SS. Optical characterization of NIPAM and PAGAT polymer gels for radiation dosimetry. *Iranian Journal of Medical Physics*. 2014;11(3-4):188-94.
28. Oldham M, editor. Optical-CT scanning of polymer gels. Third international conference of radiotherapy gel dosimetry; 2004 Sep 13-16: Ghent University, Gent, Belgium. *J Phys: Conf Ser; IOP publishing*; 2004.p.122-135
29. Wolodzko JG, Marsden C, Appleby A. CCD imaging for optical tomography of gel radiation dosimeters. *Medical Physics*. 1999 Nov;26(11):2508-13.
30. Doran SJ, Krstajić N. The history and principles of optical computed tomography for scanning 3-D radiation dosimeters. In *Journal of Physics: Conference Series* 2006 Dec 1 (Vol. 56, No. 1, p. 005). IOP Publishing.
31. Oldham M, Siewerdsen JH, Shetty A, Jaffray DA. High resolution gel-dosimetry by optical-CT and MR scanning. *Medical physics*. 2001 Jul;28(7):1436-45.
32. Fernandes JP, Pastorello BF, de Araújo DB, Baffa O. Formaldehyde increases MAGIC gel dosimeter melting point and sensitivity. In *Journal of Physics: Conference Series* 2009 May 1 (Vol. 164, No. 1, p. 012004). IOP Publishing.
33. Shiri M, Mostaar A, Mansouri Z, Sadat-Shahabi SM. Designing and developing an in-house CCD based optical CT scanner for gel dosimetry. *Iranian Journal of Medical Physics*. 2018 Dec 1;15(Special Issue-12th. Iranian Congress of Medical Physics):6-
34. Baldock C, De Deene Y, Doran S, Ibbott G, Jirasek A, Lepage M, et al. Polymer gel dosimetry. *Physics in Medicine & Biology*. 2010 Feb 11;55(5):R1.35.
35. Low DA, Harms WB, Mutic S, Purdy JA. A technique for the quantitative evaluation of dose distributions. *Medical physics*. 1998 May;25(5):656-61.
36. Low DA, Dempsey JF. Evaluation of the gamma dose distribution comparison method. *Medical physics*. 2003 Sep;30(9):2455-64.
37. Awad SI, Moftah B, Basfer A, Almousa AA, Al Kafi MA, Eyadeh MM, Rabaeh KA. 3-D quality assurance in CyberKnife radiotherapy using a novel N-(3-methoxypropyl) acrylamide polymer gel dosimeter and optical CT. *Radiation Physics and Chemistry*. 2019 Aug 1;161:34-41.
38. Pavoni JF, Pike TL, Snow J, DeWerd L, Baffa O. Tomotherapy dose distribution verification using MAGIC-f polymer gel dosimetry. *Medical physics*. 2012 May;39(5):2877-84.
39. Yao CH, Hsu WT, Lee JJ, Hsu SM, Ma PY, Hsieh BT, Chang YJ. A characteristic study on NIPAM gel dosimetry using optical-CT scanner. *Journal of Medical and Biological Engineering*. 2014 Aug 1;34(4):327-32.
40. Oldham M, Gluckman G, Kim L, editors. 3D verification of a prostate IMRT treatment by polymer gel-dosimetry and optical-CT scanning. Third international conference on radiotherapy gel dosimetry; 2004 Sep 13-16: Ghent University, Gent, Belgium. *J Phys: Conf Ser; IOP Publishing*; 2004.p.293.
41. Chang Y, Lin J, Hsieh B, Chen C, editors. A study on the reproducibility and spatial uniformity of N-isopropylacrylamide polymer gel dosimetry using a commercial 10X fast optical-computed tomography scanner. 7th international conference on 3d radiation dosimetry (IC3DDose); 2012 Dec 4-8: Sydney, Australia. *J Phys: Conf Ser; IOP Publishing*; 2013.p.012067
42. Mahdavi M, Hosseinezhad M, Mahdavi SR. Development of an Advanced Optical Coherence Tomography System for Radiation Dosimetry. *Iran. J. Med. Phys*. 2018 Oct 1;15(4):243-50.
43. Pavoni JF, Baffa O. An evaluation of dosimetric characteristics of MAGIC gel modified by adding formaldehyde (MAGIC-f). *Radiation measurements*. 2012 Nov 1;47(11-12):1074-82.